Journal of Organometallic Chemistry 694 (2009) 2604–2610

Contents lists available at ScienceDirect

Journal of Organometallic Chemistry

journal homepage: www.elsevier.com/locate/jorganchem

Coordination chemistry of mercury-containing anticrowns. Synthesis and structures of the complexes of cyclic trimeric perfluoro-*o*-phenylenemercury with ethanol, THF and bis-2,2′-tetrahydrofuryl peroxide

I.A. Tikhonova, K.I. Tugashov, F.M. Dolgushin, A.A. Korlyukov, P.V. Petrovskii, Z.S. Klemenkova, V.B. Shur *

A.N. Nesmeyanov Institute of Organoelement Compounds, Russian Academy of Sciences, Vavilov Street 28, 119991 Moscow, Russia

ARTICLE INFO

Article history:
Received 18 December 2008
Received in revised form 25 March 2009
Accepted 27 March 2009
Available online 5 April 2009

Keywords:
Anticrowns
Alcohols
Complexes
Ethers
Peroxides
Polymercuramacrocycles

ABSTRACT

Cyclic trimeric perfluoro-*o*-phenylenemercury (o-$C_6F_4Hg)_3$ (**1**) is capable of reacting with ethanol to form a 1:1 complex, {[(o-$C_6F_4Hg)_3$](EtOH)} (**2**), having a pyramidal structure. The ethanol molecule in **2** is coordinated through the oxygen atom to all Hg atoms of the macrocycle. The interaction of **1** with THF followed by drying of the product obtained in vacuum also gives the corresponding pyramidal 1:1 complex {[(o-$C_6F_4Hg)_3$](THF)} (**3**). However, when a THF solution of **1** is slowly concentrated to a small volume and the resulting crystals are not dried, three cocrystallized adducts, viz., {[(o-$C_6F_4Hg)_3$](THF)$_2$} (**4**), {[(o-$C_6F_4Hg)_3$](THF)$_3$} (**5**) and {[(o-$C_6F_4Hg)_3$](THF)$_4$} (**6**), containing two, three and even four THF molecules, respectively, are produced. Complex **4** has a bipyramidal structure. Complexes **5** and **6** are also characterized by the presence of a bipyramidal fragment formed by two coordinated THF species. The topological analysis of the DFT-calculated function of the electron density distribution in the crystals of **2** and **3** revealed the critical points (3, −1) on each of the three Hg···O lines, which is in accord with the X-ray diffraction data indicating on the presence of the triply coordinated Lewis base molecule in both adducts. If a THF solution of **1** is held for a month at 20 °C on air under stirring, a sandwich complex of **1** with previously unknown bis-2,2′-tetrahydrofuryl peroxide (THFPO) is formed. The THFPO ligand in this sandwich, {[(o-$C_6F_4Hg)_3$]$_2$(THFPO)} (**7**), provides all its four oxygen atoms for the bonding to the molecules of **1**. Two of these oxygen atoms, belonging to the tetrahydrofuryl moieties, are cooperatively bound each by three Hg atoms of the neighbouring macrocyclic unit whereas two others, belonging to the peroxide group, coordinate to a single Hg atom of the adjacent macrocycle.

1. Introduction

Anticrowns [1] constitute a remarkable class of promising reagents whose coordination and catalytic chemistry has received considerable development over the last two decades (see e.g. reviews [2a–g] and papers cited in [3a–c]). Being charge-reverse analogues of conventional crown compounds, these macrocyclic multidentate Lewis acidic hosts exhibit a high activity in the binding of various anions and neutral Lewis bases to form complexes of the unique structures. The successful applications of anticrowns in catalysis [2a–c,4,5] and as ionophores for ion-selective electrodes [2b,6] have also been reported.

Among the presently known anticrowns, one of the most studied ones is cyclic trimeric perfluoro-*o*-phenylenemercury (o-$C_6F_4Hg)_3$ (**1**) [7] containing three Hg atoms in a planar nine-membered ring. For this macrocycle, a large number of complexes with different anionic and neutral Lewis basic species has been prepared [2a,c,d,3a–c]. In the majority of structurally characterized complexes, there is at least one motif wherein a molecule of a Lewis base is cooperatively coordinated by all Lewis acidic Hg sites of **1**, thereby leading to the unusual pyramidal, bipyramidal and sandwich structures or fragments.

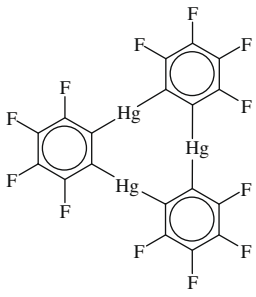

(1)

The synthesis of complexes of **1** is often carried out using THF and alcohols (MeOH, EtOH) as solvents. Because molecules of these

* Corresponding author.
E-mail address: vbshur@ineos.ac.ru (V.B. Shur).

0022-328X/$ - see front matter © 2009 Elsevier B.V. All rights reserved.
doi:10.1016/j.jorganchem.2009.03.046

solvents possess donor properties they could coordinate with the mercury anticrown and, as a consequence, compete with a Lewis basic guest for the coordination sites of **1**. The existence of such a competition is supported by ^{199}Hg NMR data which indicate that adducts of **1** with so weak Lewis bases as nitriles [8], ethyl acetate [9], nitrobenzene [3b] and some others can persist in a THF solution only in the presence of a large excess of the corresponding free Lewis basic guest.

Taking these data into account, we decided to examine the state of macrocycle **1** in THF and ethanol media, and the results of this study are described in detail below. An unusual complex **1** with bis-2,2′-tetrahydrofuryl peroxide, formed on a prolonged contact of a THF solution **1** with air, is also reported.

2. Results and discussion

Slow concentration of an ethanol solution of **1** results in the formation of a colourless crystalline solid which has been identified as a 1:1 complex of **1** with ethanol, {[(*o*-$C_6F_4Hg)_3$](EtOH)} (**2**), on the basis of elemental analysis. The isolated compound is moderately stable at room temperature and is much better soluble in CH_2Cl_2 and ether than the starting macrocycle. The IR spectrum of **2** in Nujol mull exhibits the weak ν(O–H) band at 3593 cm^{-1} shifted by 40 cm^{-1} to lower frequencies relative to the corresponding ν(O–H) band (3633 cm^{-1}) for free, non-associated EtOH [10]. The ^{1}H NMR spectrum of **2** in CD_2Cl_2 is similar in its parameters to that of free EtOH in the same solvent with the exception of the coupling constant of the CH_2 and OH protons (3.0 Hz in **2** and 5.2 Hz in EtOH).

An X-ray diffraction study of the complex has shown that it has a pyramidal structure (Fig. 1). The ethanol molecule in **2** is coordinated through the oxygen atom to all Hg atoms of the macrocycle and forms with **1** one comparatively short Hg–O distance (2.907(3) Å; see Table 1) and two somewhat longer ones (3.145(3) and 3.134(3) Å). All these distances are significantly shorter, however, than the sum of the van der Waals radii of mercury (1.73–2.00 Å [11a,b], 2.1 Å [11c]) and oxygen (1.54 Å [11d]) atoms. The C(19)–O(1) bond vector in **2** deviates from the perpendicular to the mean plane of the central nine-membered ring of **1** by 40.9°. In the crystal, molecules of **2** are associated into a complex three-dimensional structure due to shortened (as compared to the sum of the van der Waals radii) intermolecular Hg···F (3.107(3)–3.351(3) Å), Hg···C (3.444(4) and 3.446(4) Å) and C···C (3.188(6)–3.300(6) Å) contacts between the adjacent macrocyclic units (r_{vdw}(F) = 1.4 Å [11c], r_{vdw}(C_{arom}) = 1.7 Å [11c]). The H(1) atom is not involved in the formation of intermolecular hydrogen bonds O–H···O–H in the crystal structure of **2** but it forms a weak hydrogen bond with the fluorine atom of the neighbouring molecule of **2** (H(1)···F(4)$_{x,1+y,z}$ 2.42 Å, O(1)···F(4)$_{x,1+y,z}$ 3.041(4) Å, O(1)–H(1)···F(4)$_{x,1+y,z}$ 131°). The IR data also indicate on the absence of intermolecular hydrogen O–H···O–H bonds in the crystal of **2**.

When a solution of **1** in THF is evaporated at 20 °C in vacuum, a white powder of a 1:1 THF complex of **1**, {[(*o*-$C_6F_4Hg)_3$](THF)} (**3**), is produced after drying at 20 °C for 15 min. The isolated adduct is somewhat worse soluble than **2** in CH_2Cl_2 and ether but is again considerably better soluble in these solvents than **1**. The ^{1}H NMR spectrum of **3** in [D_6]acetone is practically identical to that of free THF in the same solvent. A slow evaporation of a solution of **1** in a THF–$CHCl_3$ (1:2) mixture gives crystals of **3** suitable for the X-ray diffraction study.

The structure of **3** is shown in Fig. 2. The complex has also a pyramidal structure with the THF molecule simultaneously coordinated via the oxygen atom to the three Hg atoms of **1**. Like the ethanol ligand in **2**, the THF ligand in **3** forms with **1** one comparatively short Hg–O bond (2.853(3) Å; see Table 2) and two noticeably longer ones (3.229(3) and 3.251(3) Å). The molecule of THF in **3** is in a twist conformation: the C(20) and C(21) atoms deviate from the C(19)–O(1)–C(22) plane in the opposite directions by 0.30 and 0.32 Å. In the crystal, molecules of **3** as those of **2** are associated due to shortened intermolecular Hg···F (3.136(3) and 3.285(3) Å), Hg···C (3.387(4)–3.488(4) Å) and C···C (3.133(8)–3.326(6) Å) contacts between the juxtaposed macrocycle moieties.

A quite different situation is observed when a THF solution of **1** is slowly concentrated to a small volume and the resulting crystals

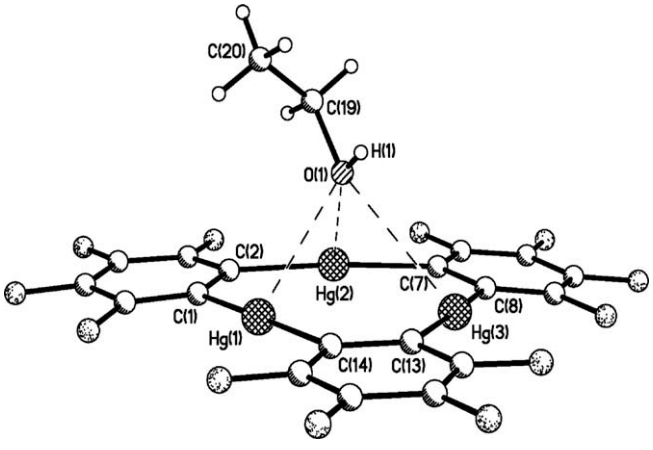

Fig. 1. Molecular structure of complex **2** in the crystal.

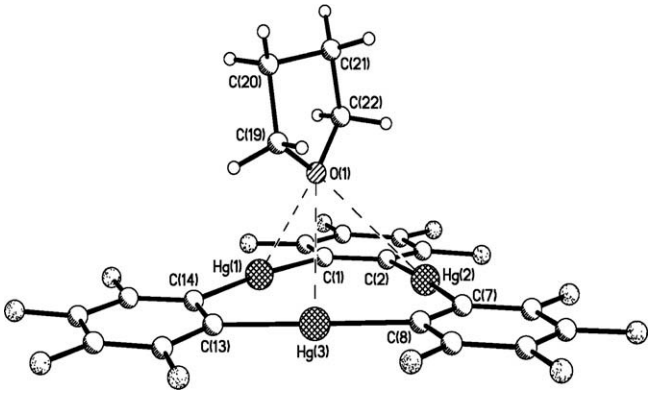

Fig. 2. Molecular structure of complex **3** in the crystal.

Table 1
Selected bond lengths (Å) and angles (°) in complex **2**.

Hg(1)–O(1)	2.907(3)	C(19)–O(1)	1.447(5)
Hg(2)–O(1)	3.145(3)	O(1)–H(1)	0.84
Hg(3)–O(1)	3.134(3)	C(19)–C(20)	1.509(6)
C(19)–O(1)–H(1)	109.5	O(1)–C(19)–C(20)	112.7(4)

Table 2
Selected bond lengths (Å) and angles (°) in complex **3**.

Hg(1)–O(1)	2.853(3)	C(22)–O(1)	1.461(5)
Hg(2)–O(1)	3.251(3)	C(19)–C(20)	1.522(6)
Hg(3)–O(1)	3.229(3)	C(20)–C(21)	1.520(6)
C(19)–O(1)	1.442(5)	C(21)–C(22)	1.494(7)
C(19)–O(1)–C(22)	108.7(3)	C(20)–C(21)–C(22)	102.1(4)
O(1)–C(19)–C(20)	105.7(3)	O(1)–C(22)–C(21)	106.3(4)
C(19)–C(20)–C(21)	102.1(4)		

Table 3
The Hg–O bond lengths (Å) in complexes **4**–**6**.

Complex ***4***			
Hg(1A)–O(1)	3.157(7)	Hg(1A)–O(2)	2.897(7)
Hg(2A)–O(1)	2.874(6)	Hg(2A)–O(2)	3.335(7)
Hg(3A)–O(1)	3.335(7)	Hg(3A)–O(2)	3.215(7)
Complex ***5***			
Hg(1B)–O(3)	2.924(7)	Hg(2B)–O(4)	2.877(6)
Hg(2B)–O(3)	3.273(8)	Hg(3B)–O(4)	3.339(6)
Hg(3B)–O(3)	3.343(7)	Hg(3B)–O(5)	3.621(9)
Hg(1B)–O(4)	3.128(7)		
Complex ***6***			
Hg(1C)–O(6)	2.957(7)	Hg(2C)–O(7)	3.215(8)
Hg(2C)–O(6)	2.977(8)	Hg(3C)–O(7)	3.189(8)
Hg(3C)–O(6)	3.430(7)	Hg(3C)–O(8)	3.029(11)
Hg(1C)–O(7)	3.138(7)	Hg(3C)–O(9)	3.062(12)

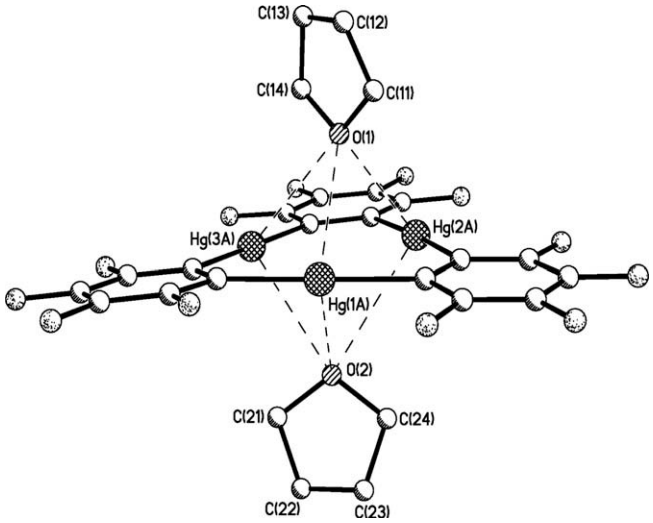

Fig. 3. Molecular structure of complex **4** in the crystal. The hydrogen atoms of the THF ligands are omitted for clarity.

Table 4
Selected bond lengths (Å) and angles (°) in complex **7**.

Hg(1)–O(1)	2.999(5)	C(19)–O(2)	1.403(8)
Hg(2)–O(1)	3.050(5)	O(2)–O(2A)[a]	1.488(9)
Hg(3)–O(1)	3.475(5)	C(19)–C(20)	1.528(9)
Hg(2)–O(2A)[a]	3.007(5)	C(20)–C(21)	1.529(10)
C(19)–O(1)	1.420(8)	C(21)–C(22)	1.505(10)
C(22)–O(1)	1.448(9)		
C(19)–O(1)–C(22)	105.3(5)	O(1)–C(19)–C(20)	107.2(6)
C(19)–O(2)–O(2A)[a]	106.5(5)	C(19)–C(20)–C(21)	104.6(6)
O(1)–C(19)–O(2)	112.5(5)	C(20)–C(21)–C(22)	101.6(6)
O(2)–C(19)–C(20)	106.0(6)	O(1)–C(22)–C(21)	104.6(6)

[a] Symmetry transformation $-x+1, -y+1, -z+1$ was used to generate equivalent atoms.

are not dried. Here, a 1:1:1 mixture of three cocrystallized complexes, $\{[(o\text{-}C_6F_4Hg)_3](THF)_2\}$ (**4**), $\{[(o\text{-}C_6F_4Hg)_3](THF)_3\}$ (**5**) and $\{[(o\text{-}C_6F_4Hg)_3](THF)_4\}$ (**6**), containing two, three and four THF molecules, respectively, is obtained. The complexes are unstable and readily transformed into complex **3** on drying in vacuum at room temperature.

According to the X-ray diffraction data, complex **4** has a bipyramidal structure (Fig. 3). The THF ligands in **4** are disposed on different sides of the metallacycle plane and each of them is cooperatively coordinated through the oxygen atom by all Lewis acidic Hg sites of **1**. The Hg–O bond distances in **4** (2.874(6)–3.335(7) Å, av. 3.14 Å; see Table 3) are comparable with those in **3** (av. 3.11 Å). Each of the THF molecules in **4** forms again one relatively short and two longer Hg–O bonds with the macrocycle.

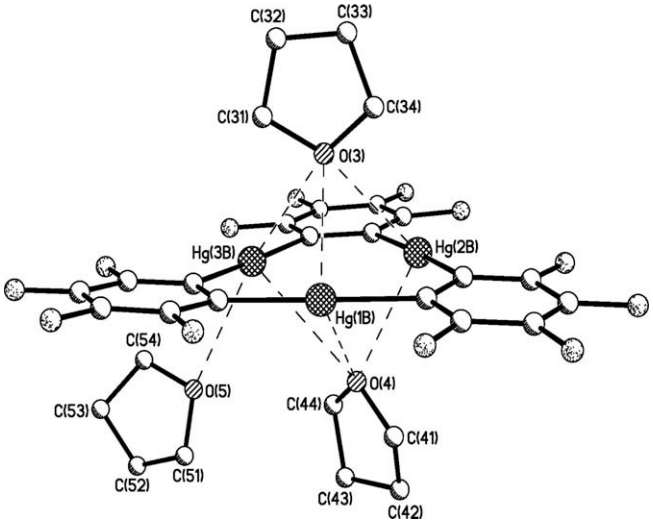

Fig. 4. Molecular structure of complex **5** in the crystal. The hydrogen atoms of the THF ligands are omitted for clarity.

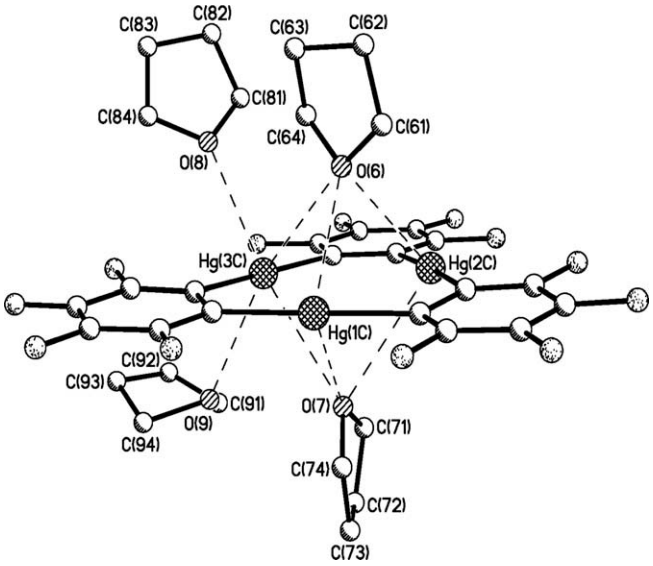

Fig. 5. Molecular structure of complex **6** in the crystal. The hydrogen atoms of the THF ligands are omitted for clarity.

Complex **5** (Fig. 4) also contains a bipyramidal fragment formed by two of the three THF ligands (Hg–O 2.877(6)–3.343(7) Å, av. 3.15 Å; see Table 3). The third THF molecule in **5** interacts very weakly, if any, with a single Hg atom of **1** (Hg–O 3.621(9) Å).

An analogous bipyramidal structural unit, formed by two of the four THF species, is present in complex **6** (Hg–O 2.957(7)–3.430(7) Å, av. 3.15 Å; see Fig. 5 and Table 3). The other two THF molecules in **6** are located above and below the plane of the anti-crown and coordinated each to a single Hg site (Hg–O 3.029(11) and 3.062(12) Å). The complex of the analogous composition and close structure has previously been isolated from the reaction of **1** with dimethyl sulfide [12]. In this complex two singly coordinated molecules of a Lewis base are bound to different Hg atoms of the macrocycle rather than to one and the same Hg site as in the case of **6**. Like **6**, the dimethyl sulfide adduct readily loses three of four Lewis basic species, giving rise to the corresponding 1:1

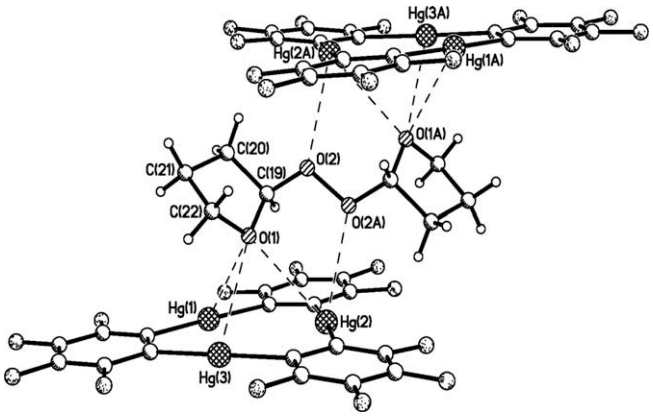

Fig. 6. Molecular structure of complex **7** in the crystal.

complex, having, however, an extended polydecker sandwich structure.

In one of the experiments on the complexation of THF with **1**, a THF solution of the starting macrocycle was held at 20 °C for a month on air, and it turned out unexpectedly that under such conditions a complex of **1** with previously unknown bis-2,2′-tetrahydrofuryl peroxide (THFPO) is formed. According to elemental analysis, the complex has the composition $\{[(o\text{-}C_6F_4Hg)_3]_2(THFPO)\}$ (**7**), i.e., contains one THFPO molecule per two molecules of the anticrown. The ^1H NMR spectrum of **7** in $[D_6]$acetone shows a doublet of doublets for the methyne proton and three distinct multiplets for the protons of the CH_2 groups. The complex is readily soluble in THF and poorly soluble in CH_2Cl_2 and Et_2O.

Fig. 6 shows the structure of **7**. The complex occupies in the crystal a special position on an inversion centre located on the midpoint of the O(2)–O(2A) bond and represents a double-decker sandwich. The THFPO ligand in **7** is arranged between the mutually parallel planes of the macrocycles and provides all its four oxygen atoms for the bonding to the molecules of **1**. The two of these oxygen atoms, belonging to the tetrahydrofuryl moieties, are cooperatively bound each by the three Hg atoms of the neighbouring macrocyclic unit (Hg–O 2.999(5)–3.475(5) Å, av. 3.18 Å; see Table 4) whereas the two others, belonging to the peroxide group, coordinate to a single Hg atom (Hg–O 3.007(5) Å). All Hg–O bond distances in **7** are again within the sum of the van der Waals radii of mercury and oxygen atoms.

The C(19), O(2), (O2A) and C(19A) atoms in **7** are coplanar. The O(2)–O(2A) distance (1.488(9) Å) is close to the average O–O bond length in free peroxides (1.482 Å [13]). The tetrahydrofuryl fragments in the complex adopt an envelope conformation: the C(22) and C(22A) atoms deviate from the O(1)C(19)C(20)C(21) and O(1A)C(19A)C(20A)C(21A) mean planes, respectively, by 0.58 Å. The mutual arrangement of these fragments corresponds to a transoid conformation. The projections of the centroids of the macrocycles onto the plane parallel to these cycles are shifted relative to each other by 5.16 Å.

The crystal packing of complex **7** can be described as consisting of extended ladder-like chains with shortened intermolecular Hg···F (3.324(4) Å), Hg···C (3.289(7)–3.533(7) Å) and C···C (3.14(1)–3.38(1) Å) contacts between the neighbouring macrocycle moieties. The chains are disposed along the [0 0 1] crystallographic direction and are linked with one another through shortened intermolecular C···C contacts (3.27(1) Å). The projections of the centroids of two adjacent macrocycles in the chain onto the plane parallel to these cycles are shifted with respect to one another by 4.57 Å, and the distance between the mean planes of the central Hg_3C_6 rings of these macrocycles is 3.25 Å. The formation of similar extended ladder-like chains (with shortened intermolecular Hg···F and Hg···C contacts) was earlier observed in the crystal packing of the 2:2 sandwich complex of **1** with maleic anhydride [5].

The complexation of **1** with ethanol, THF and THFPO does not change essentially the geometry of the macrocycle. The C–Hg–C bond angles in **2**–**7**, as in **1**, are close to 180°. The Hg–C bond lengths within the central nine-membered ring of **1** in **2**–**7** are unexceptional and range from 2.057(8) to 2.096(8) Å.

To study the electron structure of the above adducts of **1** with ethanol and THF in the crystal, the quantum chemical calculations of crystal structures of 1:1 complexes **2** and **3** have been carried out by DFT method. The optimized geometries of **2** and **3** (Table 5) reproduce with a sufficient accuracy those determined by X-ray diffraction. The discrepancies between the experimental and calculated geometries of the complexes do not exceed 0.03 Å. The most pronounced differences are observed for the intermolecular F···F and H···F distances but they do not exceed 0.1 Å. Consequently, the DFT-calculated electron density distribution function $\rho(r)$ in the crystals of **2** and **3** appeared to be well-suited for detailed investigation of the bonding pattern in these adducts.

The analysis of valence electron density distribution were performed using electron localization function (ELF) which can visualize the concentration of $\rho(r)$ in the regions of chemical bonds and lone electron pairs. As seen from Figs. 7 and 8, ELF maxima in **2** are located in the regions of the Hg–C and O–H bonds as well as in the expected positions of the lone electron pairs of the O(1) atom. One

Table 5
Selected calculated bond lengths (Å) and angles (°) in complexes **2** and **3**.

	2	**3**
Hg(1)–O(1)	2.910	2.872
Hg(2)–O(1)	3.240	3.249
Hg(3)–O(1)	3.239	3.243
C(19)–O(1)	1.451	1.457
C(22)–O(1)	–	1.458
Hg–C	2.101[a]	2.102[a]
C(1)–Hg(1)–C(14)	176.1	175.0
C(2)–Hg(2)–C(7)	174.5	175.5
C(3)–Hg(3)–C(13)	174.6	175.4

[a] Averaged value.

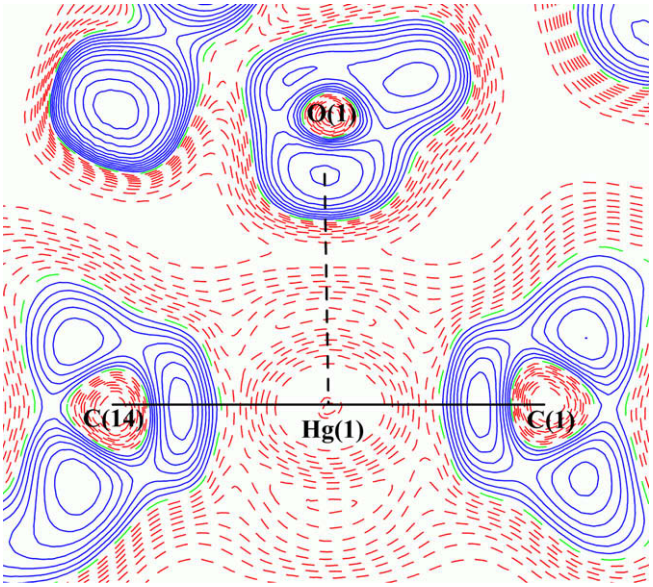

Fig. 7. The section of ELF function in the O(1)Hg(1)C(1) plane of complex **2**. The regions of valence electron density concentrations ($\eta > 0.5$) are shown by solid line. Contours are drawn at 0.05 step.

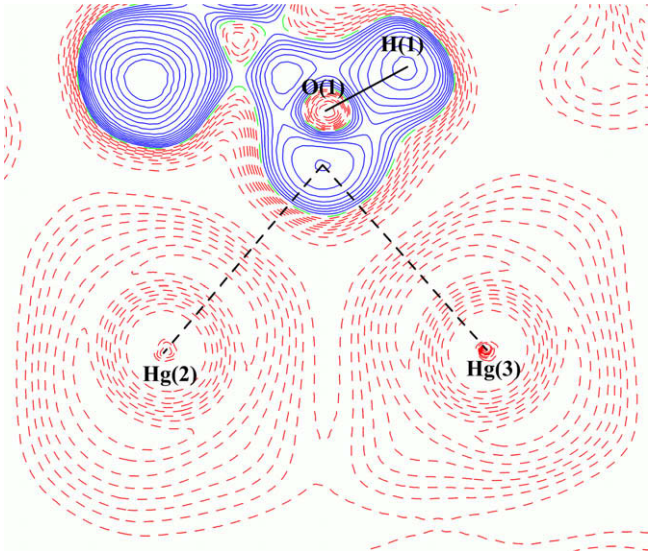

Fig. 8. The section of ELF function in the O(1)Hg(2)Hg(3) plane of complex **2**. The regions of valence electron density concentrations ($\eta > 0.5$) are shown by solid line. Contours are drawn at 0.05 step.

Table 6
Calculated topological parameters for selected bonds in the molecules of **2** and **3** in the crystal.

Bond	$\rho(r)$ (e Å^{-3})	$\nabla^2\rho(r)$ (e Å^{-5})	$E^e(r)$ (Hartree Å^{-3})	$V^e(r)$ (a.u.)	E_{bond} (kcal mol^{-1})
Complex ***2***					
Hg(1)–O(1)	0.12	1.58	0.01	−0.01	4.01
Hg(2)–O(1)	0.06	0.80	0.01	−0.005	1.53
Hg(3)–O(1)	0.06	0.76	0.01	−0.005	1.51
Hg–C	0.87[a]	0.87[a]	−0.53[a]	−0.21[a]	64.54[a]
Complex ***3***					
Hg(1)–O(1)	0.14	1.67	0.01	−0.01	4.55
Hg(2)–O(1)	0.06	0.76	0.01	−0.005	1.51
Hg(3)–O(1)	0.06	0.79	0.01	−0.005	1.52
Hg–C	0.87[a]	0.87[a]	−0.54[a]	−0.21[a]	64.81[a]

[a] Averaged value.

of the oxygen lone electron pairs is located along the Hg(1)···O(1) line whereas another one is directed approximately toward the middle of the C(7)–C(8) bond and is periplanar to the Hg(3)–C(8) and Hg(2)–C(7) bonds (the corresponding pseudotorsion angles are equal to 2.0° and 3.4°). The similar distribution of ELF is observed for complex **3**.

The detailed study of the nature of chemical bonds as well as weak intermolecular interactions in the crystals of **2** and **3** was carried out in terms of Bader's topological theory "Atoms in molecules" (AIM) [14]. The topological analysis of $\rho(r)$ revealed the critical points (CP) (3, −1) in the region of all chemical bonds in macrocycle **1** and the guest EtOH and THF molecules. It is of particular importance that the CPs(3, −1) in **2** and **3** are found also on each of the three Hg···O lines, which is in accord with the X-ray diffraction data indicating on the presence of the triply coordinated Lewis base molecule in both adducts.

The CPs(3, −1) of the C–C, C–O, C–H and O–H bonds are characterized by negative values of laplacian of $\rho(r)$ ($\nabla^2\rho(r)$) and local energy density ($E^e(r)$) that corresponds to shared type of interatomic interactions in terms of AIM theory. The Hg–C bonds are interactions of the intermediate type because positive values of $\nabla^2\rho(r)$ and negative ones of $E^e(r)$ were found in the corresponding CPs(3, −1) (Table 6). Finally, all Hg–O bonds in terms of AIM theory can be treated as closed shell interactions ($\nabla^2\rho(r)$ and $E^e(r) > 0$) that means domination of electrostatic rather than covalent interactions (cf. [15]).

AIM theory allowed one also to estimate the strength of the coordination bonds and the weak interatomic interactions in **2** and **3** using the known correlation between a bond energy and a value of potential energy density ($V^e(r)$) in the corresponding CPs(3, −1) [16].

$$E_{bond} = -1/2V^e(r)[\text{a.u.}]$$

The energy of the Hg–C bonds in **2** and **3** (av. 64.54 and 64.81 kcal mol^{-1}; Table 6) estimated in terms of the above correlation is in good agreement with the literature data for CH_3HgCl (67(3) kcal mol^{-1} [17]). The energy of the Hg(1)–O(1) coordination bond amounts to 4.01 and 4.55 kcal mol^{-1} in **2** and **3**, respectively. The Hg(2)–O(1) and Hg(3)–O(1) bonds are much weaker (ca. 1.5 kcal mol^{-1}; Table 6). The total energy of all Hg–O interactions is equal to 7.05 kcal mol^{-1} for **2** and 7.58 kcal mol^{-1} for **3**. In accordance with the X-ray diffraction data, the calculated crystal structures of **2** and **3** contain also a large number of weak intermolecular Hg···F, C···C, Hg···C and H···F (in the case of **2**) interactions.

3. Conclusion

The results of our study demonstrate that macrocycle **1** is indeed present in ethanol and THF solutions in a form of complexes with solvent molecules. In the case of ethanol, 1:1 complex **2**, having a pyramidal structure, has been isolated. In the case of THF, four complexes (**3**–**6**) containing one, two, three and even four THF ligands are produced. Complexes **3** and **4** have pyramidal and bipyramidal structures, respectively. In complexes **5** and **6**, two THF species form with **1** a bipyramidal fragment whereas the other molecules of THF interact with a single Hg atom. One may suggest that in these solvents there exists an equilibrium between complexes of **1** with different amount of the coordinated ethanol and, correspondingly, THF species (up to eight). Complexes of THF with anticrowns have earlier been obtained for the four-mercury macrocycles: $[o\text{-}C_6H_4HgOC(O)(CF_2)_3C(O)OHg]_2$ [2f] and $(o\text{-}C_2B_{10}H_{10}Hg)_4$ [2b,g]. Each of the THF species in these complexes coordinates only with one or two Hg atoms of the cycle, respectively. As concerns complexes of anticrowns with alcohols, they have not been described by now.

A prolonged contact of a THF solution of **1** with air results in the formation of a sandwich complex of **1** with THFPO. In this adduct, all four oxygen atoms of the THFPO ligand are involved in the bonding to the anticrown molecules. As is known, THF like other cyclic and acyclic ethers is able to undergo the autoxidation on air at room temperature to afford the corresponding hydroperoxide ROOH (R = 2-tetrahydrofuryl) [18,19]. The process proceeds according to radical-chain mechanism including as the rate-determining step the hydrogen atom abstraction from THF by the intermediate peroxyl radical ROO· [20].

$$R^{\cdot} + O_2 \rightarrow ROO^{\cdot}$$
$$ROO^{\cdot} + RH \rightarrow ROOH + R^{\cdot}$$

On the basis of these data, one may assume that the formation of THFPO and, correspondingly, complex **7** during the autoxidation of THF in the presence of **1** is due apparently to the coordination of the intermediate radicals R· and/or ROO· through the oxygen atom(s) with the mercury atoms of the anticrown. Such a coordination would lead to an increase in the stability and life time of these short-lived species, thereby favouring their recombination to yield THFPO and **7**. The coordinated R· and ROO· radicals could also form

in this system directly from complexes **3**–**6**. The ability of **1** to bind radical species has recently been demonstrated on the example of the reactions of **1** with nitroxide radicals [15].

4. Experimental

The starting macrocycle **1** was synthesized according to the published procedure [7a]. Solvents (EtOH, THF, $CHCl_3$) were purified by conventional methods and freshly distilled prior to use. The IR spectra were recorded as Nujol mulls on a Nicolet Magna-IR 750 Series II Fourier spectrometer. The ^1H NMR spectra were registered on a Bruker AMX-400 instrument.

4.1. Synthesis of complex *2*

Macrocycle **1** (0.1045 g, 0.1 mmol) was dissolved in 2 ml of dry ethanol and the resulting solution was allowed to slowly evaporate at 20 °C to 0.5 ml. After 2 days, the precipitated colourless crystals of complex **2** were filtered off and dried for 1 h at 20 °C in vacuum. The yield of **2** was 0.0681 g (62%). Anal. Calc. for $C_{20}H_6F_{12}Hg_3O$: C, 22.00; H, 0.55; F, 20.88. Found: C, 21.86; H, 0.57; F, 21.17%. IR (ν_{OH}, cm^{-1}, Nujol mull): 3593 (w). ^1H NMR (a saturated, ca. 0.042 M solution in CD_2Cl_2, 20 °C, 400.13 MHz, δ, ppm): 3.65 (qd, 2H, ^3J = 6.9 Hz, ^3J = 3.0 Hz, CH_2), 1.32 (br, 1H, OH), 1.19 (t, 3H, ^3J = 6.9 Hz, CH_3). ^1H NMR of free ethanol (a 0.042 M solution in CD_2Cl_2, 20 °C, 400.13 MHz, δ, ppm): 3.66 (qd, 2H, ^3J = 7.0 Hz, ^3J = 5.2 Hz, CH_2), 1.30 (t, 1H, ^3J = 5.2 Hz, OH), 1.19 (t, 3H, ^3J = 7.0 Hz, CH_3).

4.2. Synthesis of complex *3*

Macrocycle **1** (0.1049 g, 0.1 mmol) was dissolved in a Schlenk tube in 3 ml of dry THF under Ar and the resulting solution after 1 h was evaporated in vacuum. The subsequent drying of the solid residue for 15 min at 20 °C in vacuum gave a white powder of complex **3**. The yield of **3** was 0.1084 g (97%). Anal. Calc. for $C_{22}H_8F_{12}Hg_3O$: C, 23.63; H, 0.72; F, 20.39. Found: C, 23.98; H, 0.73; F, 20.27%. ^1H NMR ([D_6]acetone, 20 °C, 400.13 MHz, δ, ppm): 3.62 (m, 4H, CH_2O), 1.79 (m, 4H, CH_2). For obtaining crystals of **3** suitable for the X-ray analysis, a solution of **1** in 3 ml of a dry THF–$CHCl_3$ mixture (1:2) was allowed to slowly evaporate to 0.5 ml. In the next day, the precipitated colourless crystals were filtered off and dried in vacuum at 20 °C for 2 h. The yield of **3** was 0.0867 g (78%). Anal. Calc. for $C_{22}H_8F_{12}Hg_3O$: C, 23.63; H, 0.72; F, 20.39. Found: C, 23.11; H, 0.42; F, 20.66%. ^1H NMR ([D_6]acetone, 20 °C, 400.13 MHz, δ, ppm): 3.62 (m, 4H, CH_2O), 1.78 (m, 4H, CH_2).

4.3. Synthesis of complexes *4*–*6*

Compound **1** (0.1039 g, 0.1 mmol) was dissolved in 3 ml of dry THF and the resulting solution was allowed to slowly evaporate to 0.5 ml. Within one day, colourless crystals of cocrystallized complexes **4**–**6** were formed in the solution according to the X-ray diffraction study. Drying of **4**–**6** for 3 h at 20 °C in vacuum led to the loss of six coordinated THF molecules to afford complex **3**. The yield of **3** was 0.0712 g (64%). Anal. Calc. for $C_{22}H_8F_{12}Hg_3O$: C, 23.63; H, 0.72. Found: C, 23.10; H, 0.50%.

4.4. Synthesis of complex *7*

Macrocycle **1** (0.1048 g, 0.1 mmol) was dissolved in 5 ml of dry THF, and the resulting solution was stirred for a month on air at 20 °C in a closed system, opening it periodically twice a day for a minute. Then, the reaction mixture was concentrated to 0.5 ml, treated with 2 ml of CH_2Cl_2 and 3 ml of ether and allowed again to slowly evaporate to 0.5 ml. In the next day, the precipitated colourless crystals of complex **7** were filtered off, washed with CH_2Cl_2 (0.5 ml) and ether (3 × 1 ml) and dried for 4 h at 20 °C in vacuum. The yield of **7** was 0.0196 g (17%). Anal. Calc. for $C_{44}H_{14}F_{24}Hg_6O_4$: C, 23.32; H, 0.62; F, 20.12. Found: C, 23.43; H, 0.70; F, 19.90%. ^1H NMR ([D_6]acetone, 20 °C, 400.13 MHz, δ, ppm): 5.63 (dd, 2H), 3.80–3.85 (m, 4H), 1.85–2.00 (m, 4H), 1.65–1.80 (m, 4H).

4.5. X-ray diffraction study

Crystals of complexes **2**, **3** and **7** for the X-ray diffraction study were obtained as described above but were not dried in vacuum. Crystals of cocrystallized complexes **4**–**6** were not dried in vacuum as well. Details of crystal data, data collection and structure refinement parameters for **2**–**7** are given in Table 7. Single-crystal X-ray

Table 7
Crystal data, data collection and structure refinement parameters for **2**–**7**.

	2	**3**	**4–6**	**7**
Formula	$C_{20}H_6F_{12}Hg_3O$	$C_{22}H_8F_{12}Hg_3O$	$C_{26}H_{16}F_{12}Hg_3O_2$, $C_{30}H_{24}F_{12}Hg_3O_3$, $C_{34}H_{32}F_{12}Hg_3O_4$	$C_{44}H_{14}F_{24}Hg_6O_4$
Molecular weight	1092.02	1118.05	3786.79	2266.09
Crystal size (mm^3)	0.44 × 0.18 × 0.12	0.40 × 0.28 × 0.24	0.32 × 0.14 × 0.12	0.30 × 0.14 × 0.05
Crystal system	Triclinic	Triclinic	Triclinic	Triclinic
Space group	$P\bar{1}$	$P\bar{1}$	$P\bar{1}$	$P\bar{1}$
a (Å)	7.8975(4)	9.1335(5)	15.8364(11)	9.0599(8)
b (Å)	9.0753(4)	9.2232(5)	17.8667(13)	9.1573(8)
c (Å)	15.6356(8)	14.8934(8)	17.9525(13)	13.8361(12)
α (°)	76.060(1)	102.281(1)	83.737(2)	87.283(2)
β (°)	78.309(1)	102.783(1)	71.033(2)	89.755(2)
γ (°)	79.562(1)	105.491(1)	83.454(2)	77.546(2)
V ($Å^3$)	1054.69(9)	1128.69(11)	4758.4(6)	1119.61(17)
Z	2	2	2	1
ρ_{calc} (g cm^{-3})	3.439	3.290	2.643	3.361
$2\theta_{max}$ (°)	60	64	58	60
μ (Mo Kα) (cm^{-1})	218.99	204.68	145.86	206.39
Transmission factors, min/max	0.037/0.179	0.018/0.104	0.068/0.308	0.053/0.425
No. of collected reflections	27 493	22 234	77 547	14 340
No. of unique reflections (R_{int})	6132 (0.0440)	7784 (0.0343)	25240 (0.0871)	6454 (0.0403)
No. of observed reflections ($I > 2\sigma(I)$)	5665	6835	16 678	4949
No. of parameters	327	343	1294	352
R_1 (on F for observed reflections)[a]	0.0220	0.0251	0.0460	0.0328
wR_2 (on F^2 for all reflections)[b]	0.0515	0.0544	0.1012	0.0750

[a] $R_1 = \sum||F_o| - |F_c||/\sum|F_o|$.
[b] $wR_2 = \{\sum[w(F_o^2 - F_c^2)^2]/\sum[w(F_o^2)^2]\}^{1/2}$.

diffraction experiments were carried out with a Bruker SMART APEX II diffractometer [21] (graphite monochromated Mo Kα radiation, $\lambda = 0.71073$ Å, ω-scans, $T = 100$ K). Semiempirical method SADABS [22] for compounds **4**–**6** and **7** and numerical from crystal shape for **2** and **3** were applied for absorption correction. The structures were solved by direct methods and refined by the full-matrix least-squares technique against F^2 with the anisotropic displacement parameters for all non-hydrogen atoms (several disordered carbon atoms of the THF molecules in complexes **4**–**6** were refined isotropically). The H(1) atom of the OH group in complex **2** was located from Fourier difference synthesis and refined within "relaxed" riding model (rotation around the C(19)–O(1) bond is allowed by "AFIX 147" instruction to search for position with maximum electron density). The rest hydrogen atoms in **2** as well as the hydrogen atoms in **3**–**7** were placed geometrically and included in the structure factors calculation in the riding motion approximation. All calculations were performed using SHELXTL program package [23].

4.6. Details of quantum chemical calculations

The quantum chemical calculations of the molecules of **2** and **3** in the crystal were carried out using the VASP 4.6.31 code [24]. Conjugated gradient technique was used for optimizations of the atomic positions (started from the experimental data) and minimization of total energy. Projected augmented wave (PAW) method was applied to account for core electrons while valence electrons were approximated by plane-wave expansion with 400 eV cutoff [24]. Exchange and correlation terms of total energy were described by PBE [25] exchange-correlation functional. Kohn–Sham equations were integrated using Γ-point approximation. We believe that Γ-point approximation is sufficient for complexes **2** and **3** because of their large crystal unit cells. Using DFT method it is impossible to take into account dispersion interactions. For this reason, the calculated cell parameters may be systematically overestimated or underestimated up to 5%. Therefore, the experimental values of the cell parameters were used in the calculations. At a final step of our calculations, atomic displacements converged were lesser than 0.02 eV Å^{-1} while energy variations were lesser than 10^{-3} eV. In order to carry out the topological analysis of electron density distribution function in terms of AIM theory the dense FFT (fast Fourier transformation) grid was used (corresponding to cutoff 1360 eV). The latter was obtained by the separate single point calculation of optimized geometry with hard PAWs for each atom type. The topological analysis of electron density distribution function was carried out using AIM program – a part of ABINIT software package [26].

Acknowledgements

This work was supported by the Russian Foundation for Basic Research (the Project Codes 08-03-00332 and 07-03-00631), the Foundation of President of the Russian Federation (program for support of leading Russian scientific schools, Grant NSh-3019.2008.3) and the Russian Science Support Foundation (K.I.T.).

Appendix A. Supplementary data

CCDC 713219–713222 contain the supplementary crystallographic data for crystals **2**–**7**. These data can be obtained free of charge from The Cambridge Crystallographic Data Centre via www.ccdc.cam.ac.uk/data_request/cif. Supplementary data associated with this article can be found, in the online version, at doi:10.1016/j.jorganchem.2009.03.046.

References

[1] X. Yang, Z. Zheng, C.B. Knobler, M.F. Hawthorne, J. Am. Chem. Soc. 115 (1993) 193.
[2] (a) V.B. Shur, I.A. Tikhonova, in: J.L. Atwood, J.W. Steed (Eds.), Encyclopedia of Supramolecular Chemistry, Marcel Dekker, New York, 2004, p. 68;
(b) T.J. Wedge, M.F. Hawthorne, Coord. Chem. Rev. 240 (2003) 111;
(c) V.B. Shur, I.A. Tikhonova, Izv. Akad. Nauk, Ser. Khim. (2003) 2401 (Russ. Chem. Bull., Int. Ed. Engl. 52 (2003) 2539);
(d) T.J. Taylor, C.N. Burres, F.P. Gabbai, Organometallics 26 (2007) 5252;
(e) M.R. Haneline, R.E. Taylor, F.P. Gabbai, Chem. Eur. J. 21 (2003) 5188;
(f) J.D. Wuest, Acc. Chem. Res. 32 (1999) 81;
(g) M.F. Hawthorne, Z. Zheng, Acc. Chem. Res. 30 (1997) 267.
[3] (a) I.A. Tikhonova, K.I. Tugashov, F.M. Dolgushin, P.V. Petrovskii, V.B. Shur, Organometallics 26 (2007) 5193;
(b) I.A. Tikhonova, K.I. Tugashov, F.M. Dolgushin, A.A. Yakovenko, P.V. Petrovskii, G.G. Furin, A.P. Zaraisky, V.B. Shur, J. Organomet. Chem. 692 (2007) 953;
(c) I.A. Tikhonova, A.A. Yakovenko, K.I. Tugashov, F.M. Dolgushin, V.V. Novikov, M.Yu. Antipin, V.B. Shur, Organometallics 25 (2006) 6155.
[4] A.P. Zaraisky, O.I. Kachurin, L.I. Velichko, I.A. Tikhonova, G.G. Furin, V.B. Shur, J. Mol. Catal. A 231 (2005) 103.
[5] I.A. Tikhonova, F.M. Dolgushin, A.A. Yakovenko, K.I. Tugashov, P.V. Petrovskii, G.G. Furin, V.B. Shur, Organometallics 24 (2005) 3395.
[6] Z. Yan, I.A. Tikhonova, Z. Zhou, V.B. Shur, Y. Wu, Anal. Lett. 38 (2005) 377.
[7] (a) P. Sartori, A. Golloch, Chem. Ber. 101 (1968) 2004;
(b) M.C. Ball, D.S. Brown, A.G. Massey, D.A. Wickens, J. Organomet. Chem. 206 (1981) 265.
[8] I.A. Tikhonova, F.M. Dolgushin, A.I. Yanovsky, Z.A. Starikova, P.V. Petrovskii, G.G. Furin, V.B. Shur, J. Organomet. Chem. 613 (2000) 60.
[9] I.A. Tikhonova, F.M. Dolgushin, K.I. Tugashov, P.V. Petrovskii, G.G. Furin, V.B. Shur, J. Organomet. Chem. 654 (2002) 123.
[10] L.J. Bellamy, Advances in Infrared Group Frequencies, Mathuen and Co. Ltd., Bungay, Suffolk, 1968.
[11] (a) A.J. Canty, G.B. Deacon, Inorg. Chim. Acta 45 (1980) L225;
(b) P. Pyykkö, M. Straka, Phys. Chem. Chem. Phys. 2 (2000) 2489;
(c) S.S. Batsanov, Zh. Neorg. Khim. 36 (1991) 3015;
(d) S.C. Nyburg, C.H. Faerman, Acta Crystallogr., Sect. B 41 (1985) 274.
[12] M. Tsunoda, F.P. Gabbai, J. Am. Chem. Soc. 125 (2003) 10492.
[13] A.G. Orpen, L. Brammer, F.H. Allen, O. Kennard, D.G. Watson, R. Taylor, in: H.-B. Bürgi, J.D. Dunitz (Eds.), Structure Correlation, vol. 2, Weinheim, New York, 1994, p. 783.
[14] R.F.W. Bader, Atoms in Molecules. A Quantum Theory, Clarendon Press, Oxford, 1990.
[15] M.R. Haneline, F.P. Gabbai, Inorg. Chem. 44 (2005) 6248.
[16] E. Espinosa, E. Mollins, C. Lecomte, Chem. Phys. Lett. 285 (1998) 170.
[17] Y.-R. Luo, Comprehensive Book for Chemical Bond Energies, Taylor and Francis Group, Boca Raton, New York, London, 2006.
[18] A. Robertson, Nature 162 (1948) 153.
[19] H. Rein, R. Criegee, Angew. Chem. 62 (1950) 120.
[20] D.C. Nonhebel, J.C. Walton, Free Radical Chemistry. Structure and Mechanism, The University Press, Cambridge, 1974.
[21] APEX II software package, Bruker AXS Inc., 5465, East Cheryl Parkway, Madison, WI 5317, 2005.
[22] G.M. Sheldrick, SADABS, Bruker AXS Inc., Madison, WI 53719, USA, 1997.
[23] G.M. Sheldrick, SHELXTL, V. 5.10, Structure Determination Software Suite, Bruker AXS, Madison, Wisconsin, USA, 1998.
[24] (a) G. Kresse, J. Hafner, Phys. Rev. B 47 (1993) 558;
(b) G. Kresse, Thesis, Technische Universität Wien, 1993.;
(c) G. Kresse, J. Furthmuller, Comput. Mater. Sci. 6 (1996) 15;
(d) G. Kresse, J. Furthmuller, Phys. Rev. B 54 (1996) 11169.
[25] J.P. Perdew, S. Burke, M. Ernzerhopf, Phys. Rev. Lett. 77 (1996) 3865.
[26] X. Gonze, J.-M. Beuken, R. Caracas, F. Detraux, M. Fuchs, G.-M. Rignanese, L. Sindic, M. Verstraete, G. Zerah, F. Jollet, M. Torrent, A. Roy, M. Mikami, Ph. Ghosez, J.-Y. Raty, D.C. Allan, Comput. Mater. Sci. 25 (2002) 478.